# 3D HYBRID RAY-FD AND DWN-FD SEISMIC MODELING FOR SIMPLE MODELS CONTAINING COMPLEX LOCAL STRUCTURES

OPRŠAL IVO[1,2], BROKEŠOVÁ JOHANA[2,3], FÄH DONAT[1], GIARDINI DOMENICO[1]

## ABSTRACT

*Hybrid approaches find broad applications wherever all-in-one modelling of source, path, and site effects is too expensive. Our new 3D hybrid approach allows to compute the seismic wavefield in elastic isotropic models containing a complex local structure embedded in a large, but considerably simpler, regional structure. The hybrid modelling is realized in two successive steps.*

*In the $1^{st}$ step, the ray or discrete wave number (DWN) method is used to compute the seismic wavefield due to the source and simple regional structure. The complex local structure is not present. Thus, the excitation contains the source and regional path effects. The time history of this wavefield (excitation), recorded at the points of so called excitation box, is stored on a disk. The excitation box envelopes a small portion of a computational domain.*

*The $2^{nd}$ step of the hybrid method, now containing the complex local structure, is computed by finite differences (FD) inside the excitation box and its close vicinity. The excitation from the $1^{st}$ step is now used to inject the $1^{st}$ step wavefield into the $2^{nd}$ step computation. After that, the hybrid combination of the $1^{st}$ and $2^{nd}$ steps contains the source, regional path, and local structure effects at reasonably lower computational costs than in case of all-in-one modelling.*

*The 3D ray-FD method is tested on models in which the locally complex structure is the well-known Volvi lake basin, embedded in various 1D structures. The wavefield is excited by the point source situated outside the basin. Although the structure outside the excitation box may be less dimensional (2D, 1D, homogeneous), the whole problem is actually 3D due to the 3D features of the structure inside the excitation box, 3D shape of the excitation box, and arbitrary source − excitation-box configuration. Simple (1D) structures outside the excitation box allow for comparison with the alternative hybrid DWN-FD results. However the ray method is suitable for computation of 3D regional structures outside the excitation box. The results from both approaches show a very good agreement for realistic crustal and local structural models.*

1    Swiss Seismological Service, ETH-Hoenggerberg, CH-8093 Zürich, Switzerland (e-mail: ivo@seismo.ethz.ch)

2    Charles University, Faculty of Mathematics and Physics, Department of Geophysics, Ke Karlovu 3, 121 16, Prague, Czech Republic (e-mail: johana@seis.karlov.mff.cuni.cz)

3    Institute of Rock Structure and Mechanics, V Holešovičkách 41, 182 09 Prague, Czech Republic

Key words: 3D elastic finite differences, hybrid modeling, seismic waves, ray method, discrete wavenumber method (f-k), complex local structures

## 1. INTRODUCTION

Modern seismology often requires wavefield computations to be performed in models containing a complex 3D local structure surrounded by considerably simpler and smoother outer medium (here called regional structure). Due to the complexity of the local structure (multilayering, 3D features, topography, etc.), modelling techniques yielding a complete wavefield are unavoidable. Among them, the FD methods are probably the most appropriate because of their simplicity, stability, and easy implementation. All-in-one FD computation including source, path, and site effects for such models are too expensive (in terms of computer memory and time), or even impossible to be used. However, these cases may be handled with advantage by a hybrid approach combining expensive FD calculation for the complex part of the model (assumably small) and some other, more efficient method in the large, but simple, remaining parts of the whole model. Thus, such an approach benefits from the efficiency of the less demanding method while exploiting the wavefield completeness of the FD method.

First attempts by *Alterman and Karal (1968)* (simulation of seismic sources) and *Drake (1972)* were followed, for example, by *Kurkjian et al. (1994), Fäh et al. (1994), Robertsson et al. (1996), Caserta et al. (1999), Boore (1983)* and *Graves (1999)*. Many other references can be found in *Oršal and Zahradník (2002)*. These papers mainly treat such approach applied only for simpler cases where both methods used in hybrid approach are up to 2D. In other approaches, the full 3D methods were combined with stochastic modelling for high frequencies (see for example *Graves, 1999*). *Oršal et al. (1998)* exploited 3D finite-extent source and path effects combined with 2D local structure computation (see also *Zahradník and Moczo, 1996*). An inevitable inconsistency between the 3D and 2D wavefields resulted in a need for full 3D-3D hybrid calculations.

This paper represents a contribution to the 3D-3D hybrid methods. Here, the complex local structure is adjacent to the Earth surface. Either ray or DWN method is used for the cheap regional model computation. The main principles of the method are explained in Sec. 2.1. Sec. 2.2 provides the so-called replication test that is a criterion of applicability of the approach. Computational aspects of the methods used in our approach are discussed in Sec. 3. We have tested the approach on regional models ('homogeneous halfspace' and 'layered crust' model results are presented) that surround a complex Volvi Lake basin. The whole model is described and the results are shown and discussed in Sec. 4.

## 2. HYBRID METHODS

Among the methods mentioned above, there are special techniques which can 'exactly' inject previously computed wavefield into FD method. The accuracy of the hybrid methods is not limited only by the accuracy of methods used for the hybrid modelling, but also by the way of binding the methods together. For example an inevitable presence of inconsistencies between 3D nature of a point source wavefield in one step and further 2D FD computation of this wavefield in the other step of a possible hybrid method.

The principle applied in our two-step method was probably firstly described by *Alterman and Karal (1968)*. They introduced the 2D source wavefield (the 1st step) into the 2D FD computation (the 2nd step). For equivalent formulation combining various 1D and/or 2D methods see also *Kelly et.al. (1976), Levander (1989), Zahradník and Moczo (1996), Opršal et al. (1998), Robertsson and Chapman (2000), Fäh and Suhadolc (1994), Fäh et al. (1994), Bielak and Christiano (1984), Moczo et al. (1997)*, and *Cremonini et al. (1988)*. A combination of full 3D methods was recently presented by *Opršal and Zahradník (2002)* (FD-FD hybrid), *Bielak et al. (accepted)* and *Yoshimura et al. (accepted)* (FE-FE hybrid).

### 2.1 Basic principles of the presented hybrid method

Our two-step hybrid procedure combines the source and path effects computed by the ray or DWN method in the 1st step, and the site effects computed by the 3D FD in the 2nd step. The entire volume of interest is enclosed in the excitation box. Both steps are depicted in Fig. 1.

#### 2.1.1 The 1st step – background wavefield in regional structure

The 1st step can be performed by an arbitrary 3D method (FD, DWN, ray, analytical, etc.) for a regional-structure computational model. The structure and topography of the 1st step computational model are regional and they do not contain the local structural and topography details. The displacement history recorded at a double-planed excitation-box (parallel pairs of (grid)planes with one gridstep clearance in between, see Fig. 1) is stored on a disc as excitation that contains source-path information without local effects. This excitation $U_b = (u, v, w)_b$, so-called background wavefield, will be used in the 2nd step. The excitation box is double-planed in case of a 2nd order FD scheme (see Sec. 3.3). For higher-order-accuracy FD templates it would be necessary to have multi-planed excitation box.

#### 2.1.2 The 2nd step – complete wavefield

The sources from the 1st step are not present in the 2nd step, but they are fully represented by the excitation. The 2nd step is computed by 3D FD in two domains denoted in the right part of Fig. 1 as 'C' and 'S': complete $(U_c = (u, v, w)_c)$, and scattered $(U_s = (u, v, w)_s)$ wavefields, evaluated inside and outside the excitation box, respectively. The 2nd-step computational model, in terms of size, is usually only a fraction of the 1st-step model (Fig. 1). In the 2nd step, topography and local structures are present inside the excitation box. The only model change allowed outside the box is cropping the 2nd step model (from the 1st step one) and thus reducing its size. This cropping causes the loss of interaction of the scattered wavefield with the cropped parts (deeper layers or distant inhomogeneities), but these effects are usually negligible.

#### 2.1.3 Hybrid coupling

A single FD approximation is used in the whole 2nd step computation. The $U_c$ and $U_s$ wavefields are evaluated inside the C and S domains, respectively (see Fig. 1). This is

because all $U$ values entering the FD templates ($I_A$, $I_B$, $I_C$, $I_D$), representing a general FD scheme (Fig. 1), are either $U_c$ or $U_s$.

If the FD template is centered at either of the excitation boundary planes then two separate cases, represented by symbols II and III (Fig. 1), must be considered.

a) The center of the template lies in the S area on the outer excitation boundary grid plane. FD (II) evaluation is as usual, but the $U_b$ values of points lying in the C area (inner excitation boundary grid plane, on disc from the 1$^{st}$ step) are subtracted from their $U_c$ values:

$$U_s = U_c - U_b .\qquad(1)$$

After that all the input values of the FD approximation belong to the scattered wavefield $U_s$ and thus $U_s$ is evaluated by this approximation.

b) The center of the template lies in the C area on the inner excitation boundary grid plane. FD (III) evaluation is as usual, but the $U_b$ values of points lying in the S area (outer excitation boundary grid plane) are added to their $U_s$ values:

$$U_c = U_s + U_b .\qquad(2)$$

After that all the input values of the FD approximation belong to the complete wavefield $U_c$ and thus $U_c$ is evaluated by this approximation.

The hybrid coupling assures that the excitation boundary remains fully transparent in the 2$^{nd}$ step. The scattered wavefield penetrates freely out of the excitation boundary and, if reflected by an inhomogeneity, it can enter the excitation box repeatedly. The same applies for possible new sources added in the 2$^{nd}$ step.
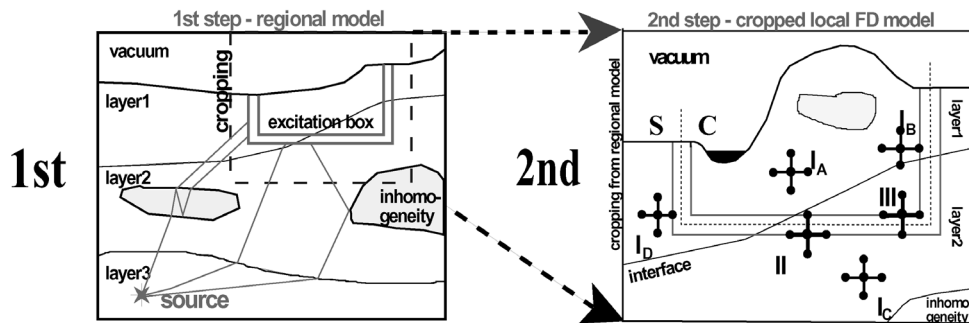


**Fig. 1.** The principle of the two-step hybrid method. The 1$^{st}$ step of the approach (left) is computed on a large simple-structure model. The time history of displacement on a formal excitation box is saved on disk. The 2$^{nd}$ step model (right) is performed on a fraction of the original model. A new local structure is inserted inside the excitation box. This box formally divides the computational domain into C and S parts, where the complete ($U_c$) and scattered ($U_s$) wavefields are computed, respectively. The former is evaluated in case the FD template is positioned as depicted by symbols $I_A$, $I_B$ and *III*, the latter in case $I_C$, $I_D$ and *II*. For further details see Sec. 2.1.3

## 2.2 Replication test

In the 2nd step, the excitation boundary provides a boundary condition in space and time for all external signals entering the excitation box in the 1st step. Therefore it is possible to perform the 2nd step computation without any model-structure change with respect to the 1st step computational model. In this case, the FD computation produces 'zero' scattered wavefield ($U_s = 0$), and the complete wavefield (inside the excitation box) should be the same as it was in the 1st step of hybrid. The complete wavefield is then equal to the background wavefield ($U_c = U_b + 0$). Thus, this replication of the wavefield can verify the consistency of coupling the 1st and 2nd step methods.

In practice, the differences between direct solution and the replication test results (inside the excitation boundary) should be as small as possible (usually less than 5% in the amplitudes). The $U_s$ in the S domain is usually $2 - 6$ orders smaller than the prevailing amplitudes inside the excitation boundary.

## 3. SOME ASPECTS OF THE METHODS USED

## 3.1 Ray method

The standard ray method is based on the zero-order high-frequency asymptotic solution of the elastodynamic equation (see, e.g., *Červený, 2001*; *Červený et al. 1977*). The wavefield described by the leading term of the ray series, is obtained along rays connecting the point source and the excitation points along the excitation box. Since rays are curves of zero thickness, such solution is, in principle, local. The wavefield in the vicinity of a ray trajectory does not influence the corresponding ray solution along the given ray. It is just a high-frequency approximation of a real wavefield.

The ray solution suffers from incompleteness of the wavefield modelled by this method, which can, in principle, contain only finite number of body waves and the waves must be 'prescribed' or 'chosen' by the user. Some wave types, even those which may be important in the wavefield, like surface waves, head waves, guided waves, diffractions on edges, near-field waves close to the source, etc., are usually not included in the ray solution. Thus, the ray method should be used only in such regions where the above mentioned waves are not too strong in amplitude, or where they arrive at times outside of the time interval of our interest.

A great disadvantage of the ray method is also that it fails at certain regions of the model (see, e.g. *Červený, 1985*), where the ray solution is either singular (e.g. vicinity of a caustic), or incorrect (overcritical reflections close to the critical point), or even not defined (shadow zones). The method is also very sensitive to fine details of the structure and thus requires smooth models where the changes of the material parameters per wavelength are small. For details on applicability of the ray method and its validity conditions see *Červený (2001), Kravstov and Orlov (1990),* and others. When used within the limits of its applicability, the ray method can provide very fast calculation of an approximate but reasonably accurate solution. The efficiency of the ray method, mainly as regards the computer time requirements, is one of its greatest advantages. The computer time demands do not increase considerably for high frequencies for which many other modelling methods (FD, DWN) become too expensive.

The ray method is conceptually simple and allows a good insight into the wavefield propagation. Individual waves (direct P and S waves, reflections from interfaces, converted waves, etc.) are computed separately and usually only a small number of these elementary waves is to be taken into account. Suitable choice of the elementary waves constituting the ray theory wavefield helps to retain the speed of the ray wavefield computations. Therefore, the method is not convenient for models with many layers separated by high contrasting interfaces where many reflected/transmitted and even multiply reflected and converted waves may play important role in the final solution.

This paper presents the hybrid ray-FD method applied to the models with very simple (even homogeneous) regional structure (see Sec. 4). Nevertheless, due to 3D features of the local structure, the excitation boundary surrounding it must be also 3D and ray tracing in such a case represents a 3D problem, i.e. 3D rays are required to be traced through the simple regional structure. For this we applied 2.5D approach proposed by *Brokešová (1993)* in which 3D rays can be computed in a general 2D structure. The approach is much more general than many approaches usually understood under the term '2.5D ray modelling', see, e.g., *Bleistein (1984)* or *Lafond and Levander (1990),* where 2D rays (in-plane) are traced in a 2D structure and only amplitudes are modified to represent a point source. Instead, in our 2.5D ray approach, the ray can be a general 3D curve with non-zero torsion, propagating in arbitrary direction through a 2D model – computations are not restricted to the plane of the symmetry of the model. In-plane ray calculations are considered as a special case. Calculation of ray trajectories utilizes the simplicity of the medium. In 2D or 1D structures, at least one slowness vector component remains constant along the whole ray and at least one ray coordinate can be computed analytically. Thus, the kinematic part of the ray calculation is simpler and more efficient than full 3D modelling. The method saves computer time needed for ray tracing and travel time computations yielding the same ray trajectories as would be obtained by a 3D ray tracer; no approximation is included. As regards the computation of ray amplitudes, in principle, the same procedures as in general 3D medium must be used, the 2.5D approach does not allow considerable simplifications in this part of the computation. Orientation of polarization vectors is to be calculated as in 3D medium as both S-wave polarization vectors may change their directions along a ray in general 2D medium when out-of-plane rays are considered. The 3D dynamic ray tracing system (see, *Červený, 2001*) is to be solved to obtain correct geometrical spreading. Slight simplifications with respect to 3D models concern only boundary conditions at interfaces (because of their 2D shape). This, however, does not contribute considerably to the efficiency of the amplitude computation.

In this paper we use two-point ray tracing (*Červený, 2001*) to obtain rays connecting the point source and the points along the excitation box. In future it would be possible to improve the hybrid approach avoiding the necessity of two-point ray tracing and utilizing interpolation between irregularly spaced ray endpoints. Two-point ray tracing is, in general, the most time consuming part of the ray calculations. However, in the particular model presented here, two-point ray tracing was very fast because of the possibility to determine ray take-of angles from the source analytically.

### 3.2 DWN method

The Discrete Wavenumber Method is based on integration (summation) in $f$ and $k$ domains (thus, also $f - k$ method) to compute the Green's functions for 1D medium composed of homogeneous layers (*Bouchon, 1981*). The DWN yields full solution given by the representation theorem (all wavetypes are included). We use the AXITRA code (*Coutant, 1989*) that utilizes the matrix method to treat the 1D model (*Kennett and Kerry, 1979*). The integration is exactly replaced by a summation thanks to artificial source periodicity. Because of that, the problem of a correct setting of integration limits is transferred to the demand of a correct truncation of the infinite summation. The summation is finished in case the sums of $n$ and $n + 1$ terms differ by less than a given value.

### 3.3 FD method

Our 3D FD method was introduced and described in *Opršal and Zahradník (2002)*. We solve the elastodynamic partial differential equation (PDE) in the time domain for Hooke's isotropic generally inhomogeneous medium with discontinuities and free-surface topography. The excitation may be point source double couple, plane wave, or arbitrary. The method is a 3D explicit FD formulation of the $2^{nd}$ order hyperbolic PDE. The accuracy in homogeneous regions is of the $2^{nd}$ order in space and time. The FD formulation is stable for high $v_p/v_s$ ratios but it has free-surface accuracy limitations for $v_p/v_s > 4$. The heterogeneous formulation uses one formula everywhere and the interface conditions are implicitly approximated via proper treatment of the discontinuous elastic parameters. This applies also for the free surface above which the parameters are zeroed (vacuum formalism). The FD method, formulated for topography models on irregular rectangular grids, is an extension of 2D P-SV case of *Opršal and Zahradník (1999)*, and 2D SH case of *Moczo (1989)*. An analogous scheme on regular grids was developed by *Moczo et al., (1999)*. Recently, 3D FD methods on irregular grids were used for example by *McLaughlin and Day (1994)*, *Pitarka (1999)* (irregular rectangular grids), and *Eisner and Clayton (2002)* (rectangular grids irregular in the vertical direction). A discontinuous-grid approach in 3D FD modeling was used by *Aoi and Fujiwara (1999)*, *Kristek et al. (1999)*, and *Pitarka (URS Corporation, personal communication, 2002)*. The irregularity of our grid is defined independently in all three dimensions by 1D vectors. The grid refinement can reduce the stair-case free-surface artifacts, and avoid oversampling of high-velocity regions. Transparent boundaries (*Emerman and Stephen, 1983*) and damping tapers (*Cerjan, 1985*) at the edges of the model are used.

## 4. NUMERICAL EXAMPLES

The excitation box is adjacent to the free surface. The size of the excitation boundary, and the parameters of the source are shown in Fig. 2. The source is a double couple with a single-sided pulse (in the force term) of maximum frequency $f_{max} = 5$ Hz and time history $\overline{f}(t)$:

$$\overline{f}(t)\big|_{t\in\langle 0,T\rangle} = \frac{T}{2\pi t}\left[-\cos\left(2\pi\frac{t}{T}\right)+\frac{1}{4}\cos\left(4\pi\frac{t}{T}\right)\right], \tag{3}$$

$$\overline{f}(t)\big|_{t\notin\langle 0,T\rangle} = 0 ,$$

where $T = 0.62$ s is duration of the signal, $T[\sec] = \dfrac{3.1}{highestfrequency[\text{Hz}]}$, *highestfrequency* is the frequency above which the absolute value of the amplitude spectrum is less than 1% of the maximum (absolute) spectral value, $t$ is time in seconds.
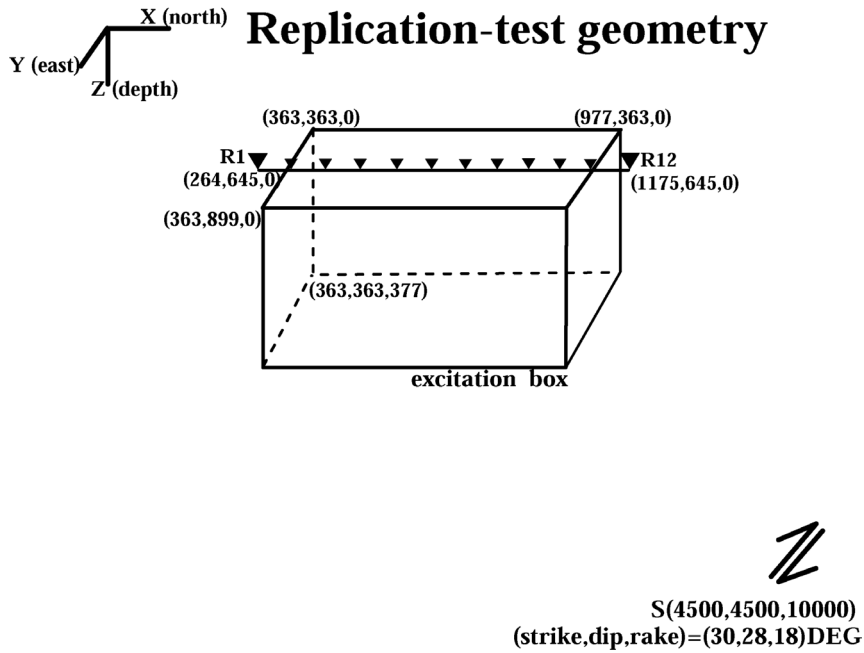


**Fig. 2.** The replication test geometry. The excitation box is adjacent to the planar free surface. Receivers R1..R12 are on the free surface. S denotes the point double-couple source. The spatial coordinates are in meters.

718

## 4.1 1ˢᵗ step − source and path effects

The 1ˢᵗ step of the hybrid computations is performed by DWN and the ray methods for two different crustal models. The 'homogeneous halfspace' model is a formal extrapolation of the Western-Greece uppermost crust layer. The parameters of the medium are shown in Fig. 3. Another model is a realistic 'layered crust' model of Western Greece (*Novotný et al., 2001*; *Novotný, Zahradník and Plicka, Charles University, Prague, personal communication, 2002*), its parameters are shown in Fig. 4.

The ray excitation for the 'homogeneous halfspace' model is realized by 6 rays: direct P, S, and the reflections/conversions from the flat free surface PP, PS, SP, SS (Fig. 3). The ray excitation for the 'layered crust' model is realized by 10 rays: direct P, S, reflections/conversions from the flat free surface PP, PS, SP, SS, and reflections/conversions PP, PS, SP, SS due to the interface in the depth of 18 km (Fig. 4).
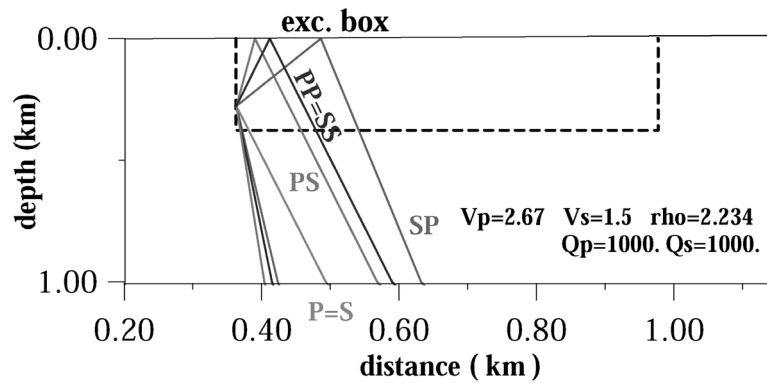


**Fig. 3.** Detail of the excitation box and the raypaths used to compute the 'halfspace model' excitation by the ray method. P = S stands for the direct waves, PP = SS represent the reflected, PS and SP the converted waves (see Sec. 4.1). The $v_p$ and $v_S$ velocities are in km/s, the density is in g/cm³, $Q_p$ and $Q_S$ are the $v_p$ and $v_S$ quality factors, respectively.
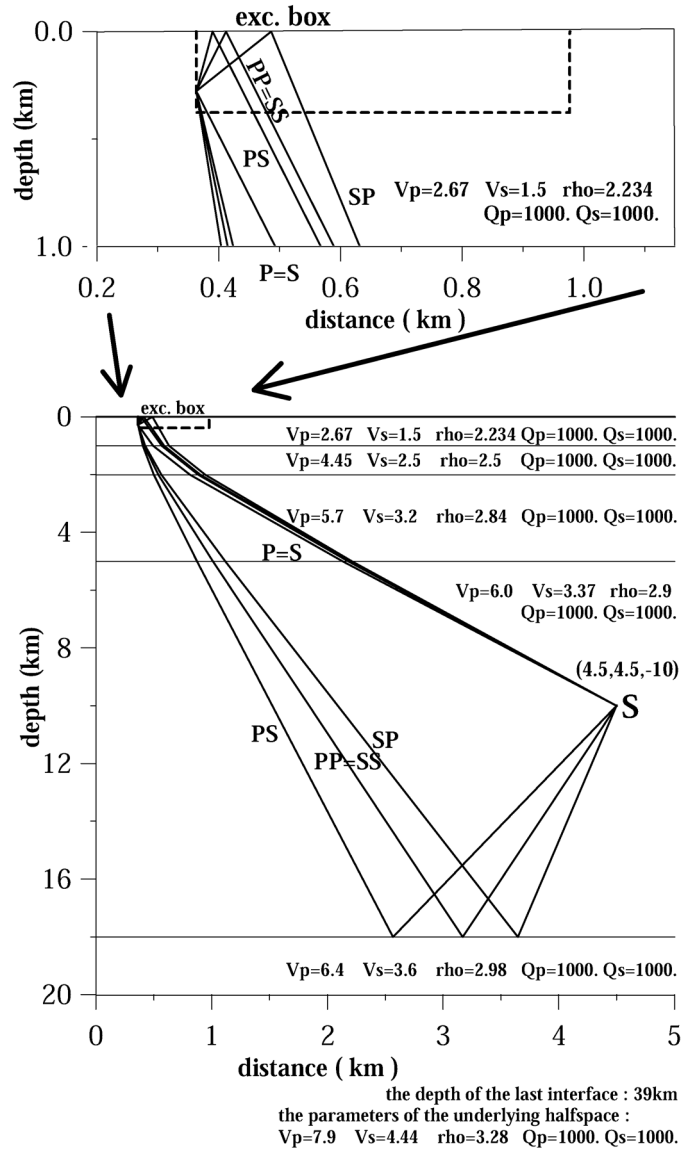
**Fig. 4.** The raypaths for the 'layered crust' model. The upper panel shows a detail near the free surface with direct P and S waves and surface reflections/conversions (PP, PS, SP, SS). The lower panel shows the layered model with direct P and S waves and the 18 km-interface reflections/conversions (PP, PS, SP, SS) (see Sec. 4.1). The $v_p$ and $v_s$ velocities are in km/s, the densities are in g/cm$^3$, $Q_p$ and $Q_s$ are the $v_p$ and $v_s$ quality factors, respectively.

### 4.2 Replication tests for 1D regional models

The replication test (the 2nd step of hybrid computation for the same model as the 1st step) is performed using ray and DWN excitations for both 'homogeneous halfspace' and 'layered crust' models. The results are compared to direct DWN solution (for a corresponding model) at 12 receivers placed on the free flat surface (Fig. 2). Inside the excitation box, the resulting wavefield should be the same as the direct solution; outside the box, the wavefield should be zero (Sec. 2.2). The results of the test are compared by 'Relative error' (*RE*). It is defined as a typical relative change in the corresponding local extremes of displacement obtained in the 1st and 2nd steps, respectively. It is only suitable for signals which are 'similar enough' to have the corresponding maxima.

'Homogeneous halfspace' model: Fig. 5 shows a very good agreement ($RE \approx 7 \times 10^{-3}$) between direct DWN and DWN-FD hybrid solution inside the excitation box. The DWN-FD values are negligibly small ($RE \approx 5 \times 10^{-4}$) at the receivers outside the excitation box (scattered wavefield), as desired (Sec. 2.2). The ray-FD hybrid shows a very good agreement with the direct DWN solution for the P-wave part of the wavefield ($RE \approx 0.015$). The S-wave part of the ray-FD is not so accurate ($RE \approx 0.2$), especially at receivers situated farther from the source. The ray-FD synthetics show low-frequency artifacts after either P and S-wave phase. The scattered ray-FD wavefield is also evident and it is stronger ($RE \approx 0.05$) at the receivers farther from the source.
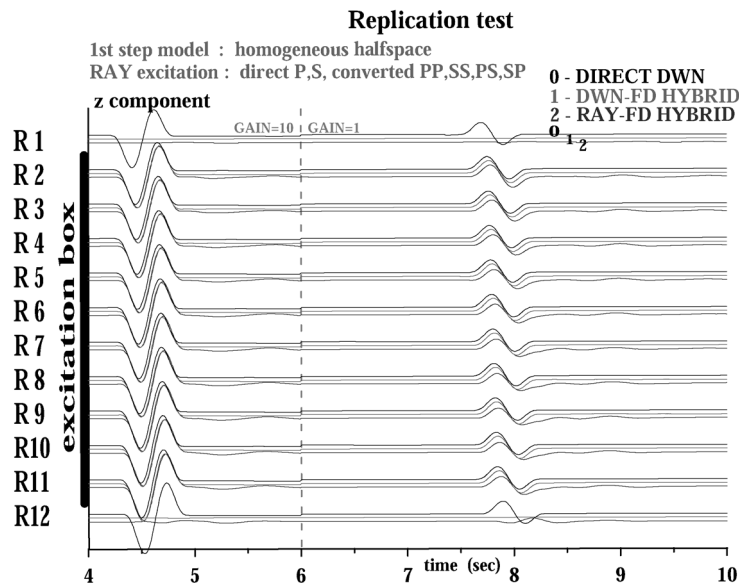


**Fig. 5.** Replication test (z component) for the 'homogeneous halfspace' model (Sec. 4.2). Direct DWN computation (trace 0) is compared to the DWN-FD (trace 1) and ray-FD (trace 2) hybrid solutions. Receivers R1-R12 are placed on the flat free surface (Fig. 2). The vertical dashed line depicts the time (6 s) before which the amplitudes of the shown synthetics are multiplied by a factor of 10.

'Layered crust' model: Fig. 6. The direct DWN wavefield evaluated for this model has relatively strong surface and guided waves. Its comparison to DWN-FD shows a very good agreement ($RE \approx 7 \times 10^{-3}$) for the whole time history at all receivers inside the excitation box. The wavefield outside the excitation box is negligibly small ($RE \approx 5 \times 10^{-4}$). The ray-FD replication shows a good agreement for the P-wave ($RE \approx 0.1$ – the first local maximum). The agreement of the S-wave part of the wavefield is less accurate ($RE \approx 0.05$ – the first pulse), the differences are visible. The Ray-FD solution is relatively simple (surface/guided waves are completely missing). The scattered ray-FD wavefield is very small ($RE \approx 0.015$) at receiver closer to the source and relatively small ($RE \approx 0.03$) at the receiver further from the source.

The discrepancies between the direct DWN and ray-FD solutions are mostly due to the lack of the surface waves in the ray excitation, and due to the incompleteness of the (local) wave solution. However, the replication test did not show substantial differences for those parts of the wavefield (e.g., P, PP, PS waves) contained in both, ray and DWN, excitations. The replication test results show that it is possible to bound the mentioned methods in hybrid computation, nevertheless it is necessary to keep in mind the limitations of these methods.
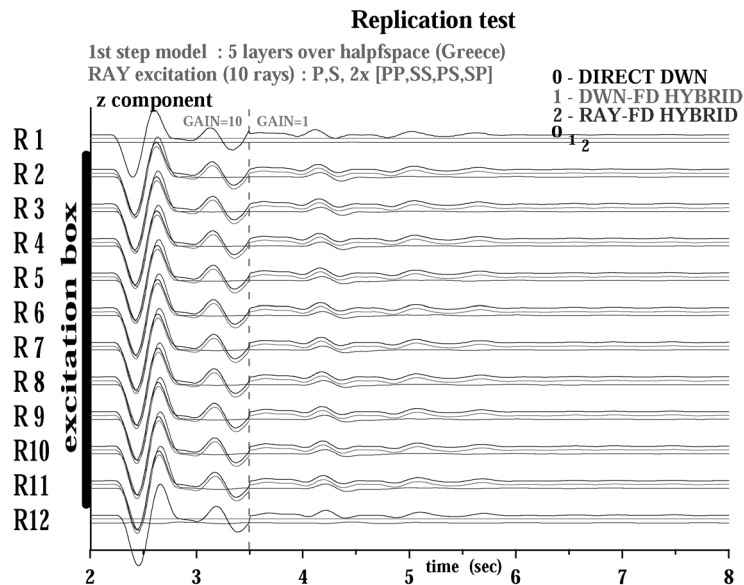


**Fig. 6.** Replication test (z component) for the 'layered crust' model (Sec. 4.2). Direct DWN computation (trace 0) is compared to the DWN-FD (trace 1) and ray-FD (trace 2) solutions. Receivers R1 – R12 are placed on the flat free surface (Fig. 2). The vertical dashed line depicts the time (3.5s) before which the amplitudes of the shown synthetics are multiplied by a factor of 10.

### 4.3 2ⁿᵈ step – source-path-site effects

The soft-sediments model in the 2nd step is the same for both hybrid computations. It is a modification of the 2D Volvi Lake basin model *(Jongmans et al., 1998)*. The modified model cross-section is depicted in Fig. 7. This cross-section is re-scaled (with factor 0.078) in the horizontal direction. A quantitative description of the material parameters is given in Table 1. To create a 3D structure, the model is formally expanded and tapered in the direction perpendicular to the above mentioned cross-section plane. Thus, this 3D Volvi-Lake model is an illustrative example of a site. The topography of the model and the line of surface receivers are depicted in Fig. 8. The large velocity and velocity-ratio contrasts present in this 2nd step model are responsible for complex interference field inside the basin.
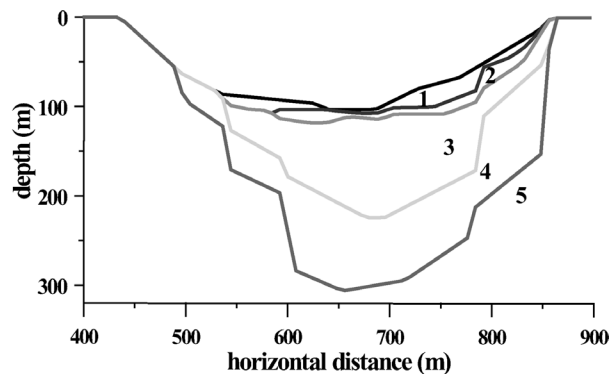


**Fig. 7.** The vertical section (x-z plane) of a simplified Volvi Lake basin structural model. The material parameters of the depicted blocks are specified in Table 1.
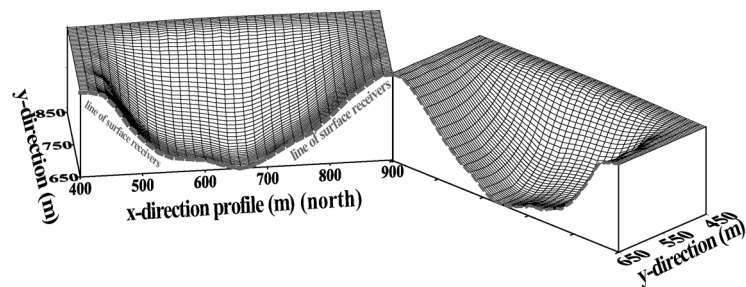


**Fig. 8.** 3D topography of the modified 2D Volvi Lake basin model. It was formally extended by tapering the 2D model in the y-direction to create a suitable 3D test model. The receivers are situated on the topographic free surface on the 'line of surface receivers'.
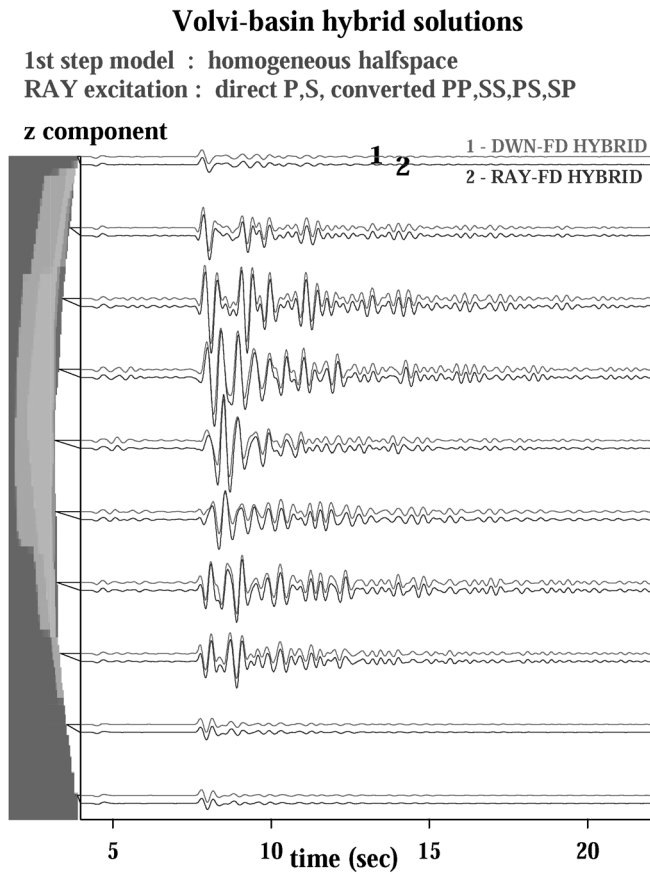
**Volvi-basin hybrid solutions**

**1st step model : homogeneous halfspace**
**RAY excitation : direct P,S, converted PP,SS,PS,SP**

**z component**



**Fig. 9.** The comparison of the DWN-FD (trace 1) and ray-FD (trace 2) hybrid solution (z component) for modified Volvi Lake basin model embedded in 'halfspace model'. It shows very good agreement. Amplification of the ground motion is apparent at the soft soil locations. The relatively weak surface waves (present in the DWN excitation) are not 'missing' in the ray-FD solution. The left part of the panel shows one slice of the computational-model (for comparison see model section in Fig. 7).
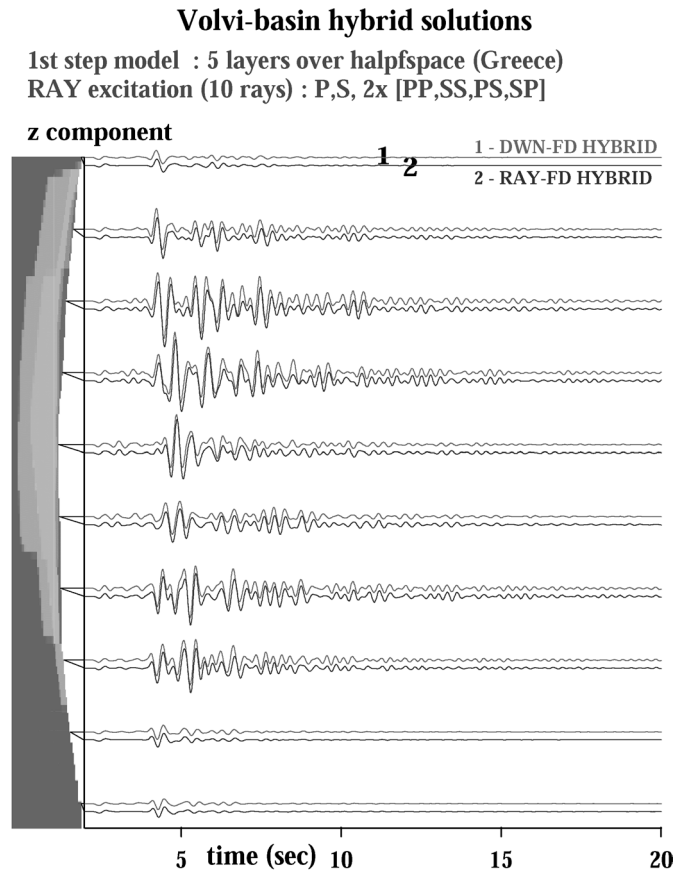
**Volvi-basin hybrid solutions**

**1st step model : 5 layers over halpfspace (Greece)**
**RAY excitation (10 rays) : P,S, 2x [PP,SS,PS,SP]**

**z component**



1 - DWN-FD HYBRID
2 - RAY-FD HYBRID

5   **time (sec)**   10   15   20

**Fig. 10.** The comparison of the DWN-FD (trace 1) and ray-FD (trace 2) hybrid solution (z component) for modified Volvi Lake basin model embedded in 'layered model'. The agreement is less accurate mainly due to the lack of the surface/guided waves in the ray excitation wavefield compared to the DWN excitation (Fig. 6). Amplification of the ground motion is apparent at the soft soil locations. The left part of the panel shows one slice of the computational-model (for comparison see model section in Fig. 7).

The hybrid-computation results for the 'homogeneous halfspace' and 'layered crust' models are shown in Figs. 9 and 10, respectively. The figures show a very good agreement between the DWN-FD the ray-FD results. The differences in the ray and DWN excitations for the 'layered crust' model (Fig. 10) have a certain influence on the resulting wavefield. For example, it is visible on the difference between the solutions at times 6 – 7 s (compare to corresponding part of the synthetics in Fig. 9 at times 9 – 11 s).

Both hybrid-computation solutions show strong site effects due to the soft soil layers. The complexity of the site effects is indicated by the difference between the synthetics computed for bedrock receiver (for example the lowermost traces in Figs. 9 and 10), and for the receivers inside the low velocity basin.

**Table 1.** Material parameters of modified Volvi basin model. The numbers of the blocks correspond to blocks in Fig. 7

| Block No. | 1 | 2 | 3 | 4 | 5 |
|---|---|---|---|---|---|
| $v_p$ (m/s) | 460 | 1500 | 1800 | 2600 | 2670 |
| $v_s$ (m/s) | 230 | 300 | 425 | 700 | 1500 |
| $\rho$ (kg/m$^3$) | 1750 | 2000 | 2075 | 2150 | 2234 |

## 4.4 Computational details

The computation of the excitation by the DWN method took about 10 hours for both models. The excitation evaluated by the ray method took about 6 minutes (6 rays, 'homogeneous halfspace') and 10 minutes (10 rays, 'layered crust'); all on a Pentium 1.4GHz. There were 2848 excitation points in the 1$^{st}$ step excitation boundary. The 2$^{nd}$ step excitation boundary consisted of 23539 FD grid points. The excitation was interpolated in space and time. The 2$^{nd}$ step computations were performed on PII 500MHz and took about 12 hours to compute. The grid was irregular in all 3 directions changing from 5 m to 33 m, the whole FD model was approximately 700000 gridpoints, and the timestep was 0.00125 s. This gives a good accuracy up to frequency of 5 Hz.

## 5. CONCLUSIONS AND PROSPECTS

A new two-step 3D hybrid methods (ray-FD, DWN-FD) have been successfully developed and tested. Satisfactory consistency tests (replication tests) have shown that combining DWN and ray methods with the FD method is applicable in principle. Because of the accuracy limitation of the 2$^{nd}$ order FD method, it will be necessary to upgrade the 2$^{nd}$ step of the hybrid approach to the 4$^{th}$ order FD method.

For a particular local site model, the DWN-FD and ray-FD gave practically the same results, however, with much different computer time requirements for the 1$^{st}$ hybrid step computation. The DWN method gives (for 1D layered models) complete wavefield containing also surface and guided waves. The advantage of the ray-FD hybrid is that it is faster and, in principle, applicable to more complex (2D, 3D) regional models. On the other hand, DWN-FD may be very useful in case of complex 1D model in the 1$^{st}$ step, as well as in case when near-field effects are of interest. The DWN-FD method would be applicable for sites where the 1D regional structure (for a given frequency) is

predominant. Our next goal is to come to 2D or 3D models composed of homogeneous blocks separated by inclined or curved interfaces, and, finally, to the 3D models containing interfaces as well as vertical and lateral gradients of material parameters.

In more complex models, it would be very useful to modify the ray part of computation avoiding two-point ray tracing and utilizing interpolation from irregularly spaced ray endpoints along or in the vicinity of excitation boundary. This would further decrease computer time demands for ray calculations.

Our final goal (mainly for the exploration seismology purposes), is to modify the hybrid approach to handle models with the locally complex structure not only adjacent to the earth's surface, but also buried inside the regional structure. This may find broad applications, e.g., in seismic prospection. In this case, the two-step hybrid approach should be replaced by a three-step one. In the third step, the FD wavefield from inside excitation boundary would be propagated towards receivers outside excitation boundary (e.g., at the surface) using some efficient method (e.g., ray method). Similar approach for 2D acoustic case was proposed by *Lecomte (1996)*, *Gjøystdal et al. (1998)*. Recently, *Gjøystdal et al. (2002)*, discussed methodically this approach as an important possibility to extend the applicability of the ray theory for models not (as a whole) optimally suited for the ray method. In these papers, the approach is illustrated on 2D acoustic models inspired from existing structures in the North Sea. The idea of the three-step ray-FD hybrid method was generalized for elastic models by *Hokstad et al. (1998)*. In our paper, we try to generalize the hybrid approach considering 3D elastic models.

## References

Alterman Z. and Karal F.C., 1968. Propagation of elastic waves in layered media by finite-difference methods. *Bull. Seismol. Soc. Am.*, **58**, 367-398.

Aoi S. and Fujiwara H., 1999. 3D Finite-difference method using discontinuous grids. *Bull. Seismol. Soc. Am.*, **89**, 918-930.

Bielak J. and Christiano P., 1984. On the effective seismic input for nonlinear soil structure interaction systems. *Earthq. Eng. Struct. Dyn.*, **12**, 107-119.

Bielak J., Loukakis K., Hisada Y. and Yoshimura C., 2002. Domain reduction method for three-dimensional earthquake modeling in localized regions. Part I: Theory. *Bull. Seismol. Soc. Am.*, accepted.

Bleistein N., 1984. *Two-and-One-Half Dimensional In-Plane Wave Propagation*. Research Report, Center of Wave Phenomena, Colorado School of Mines, Golden, Colorado.

Boore D.M., 1983. Stochastic simulation of high-frequency ground motions based on seismological models of the radiated spectra. *Bull. Seismol. Soc. Am.*, **73**, 1865-1894.

Bouchon M., 1981. A simple method to calculate Green's functions for elastic layered media. *Bull. Seismol. Soc. Am.*, **71**, 959-971.

Brokešová J., 1993. *High-Frequency Ground Motions due to Extended Seismic Sources in Complex Structures*. Ph.D. Thesis, Charles University, Prague.

Caserta A., Zahradník J. and Plicka V., 1999. Ground motion modelling with a stochastically perturbed excitation. *J. Seismol.*, **3**, 45-59.

Cerjan C., Kosloff R. and Reshef M., 1985. A nonreflecting boundary condition for discrete acoustic and elastic wave equations. *Geophysics*, **50**, 705-708.

Červený V., 1985. Ray synthetic seismograms for complex two-dimensional and three-dimensional structures. *Journal of Geophysics*, **58**, 2-26.

Červený V., 2001. *Seismic Ray Theory.* Cambridge University Press.

Červený V., Molotkov I.A. and Pšenčík I., 1977. *Ray Method in Seismology*. Charles University, Prague.

Coutant O., 1989. *Programme de simulation numerique AXITRA*. Rapport LGIT, Universite Joseph Fourier, Grenoble.

Cremonini M.G., Christiano P. and Bielak J., 1988. Implementation of effective seismic input for soil-structure interaction systems. *Earthq. Eng. Struct. Dyn.*, **16**, 615-625.

Drake L.A., 1972. Love and Rayleigh waves in nonhorizontally layered media. *Bull. seismol. Soc. Am.*, **62** , 1241-1258.

Eisner L. and Clayton R.W., 2002. Equivalent medium parameters for numerical modelling in media with near surface low velocities. *Bull. seismol. Soc. Am.*, 92, 711-722.

Emerman S.H. and Stephen R.A., 1983. Comment on "Absorbing Boundary Conditions for Acoustic and Elastic wave Equations", by R. Clayton and B. Enquist. *Bull. seismol. Soc. Am.*, **73**, 661-665.

Fäh D. and Suhadolc P., 1994. Application of Numerical Wave-Propagation Techniques to Study Local Soil Effects – The case of Benevento (Italy). *Pure Appl. Geophys.*, **143**, 513-536.

Fäh D., Suhadolc P., Mueller S. and Panza G.F., 1994. A Hybrid Method for the Estimation of Ground Motion in sedimentary Basins – Quantitative Modelling for Mexico City. *Bull. seismol. Soc. Am.*, **84**, 383-399.

Gjøystdal H., Lecomte I., Mjelva A.E., Maaø F., Hokstad K. and Johansen T.A., 1998. Fast repeated seismic modelling of local complex targets. *SEG 68th annual Meeting, Expanded Abstracts*, 1452-1455.

Gjøystdal H., Iversen E., Laurain R., Lecomte I., Vinje V. and Åstebøl K., 2002. Review of Ray Theory Applications in Modelling and Imaging of Seismic Data. *Stud. Geophys. Geod.*, **46**, 113-164.

Graves R.W., 1999. Long period 3-D finite-difference modelling of the Kobe mainshock. In: Irikura, K. et al. (eds.), The Effects of Surface Geology on Seismic Motion – Part III, Balkema, Rotterdam (*Proceedings of ESG'98, December 1-3, 1998, Yokohama, Japan*), 1339-1345.

Hokstad K., Lecomte I., Maaø F., Tuseth M., Mjelva A.E., Gjøystdal H. and Sollie R., 1998. Hybrid modelling of elastic wavefield propagation. *EAGE 60th annual Meeting, Extended Abstracts*, 5-56.

Jongmans D., Pitilakis K., Demanet D., Raptakis D., Riepl J., Horrent C., Tsokas G., Lontzetidis K. and Bard P.-Y. 1998, EURO-SEISTEST: Determination of the geological structure of the Volvi basin and validation of the basin response. *Bull. seismol. Soc. Am.*, **88**, 473-487.

Kennett B.L.N. and Kerry N.J., 1979. Seismic waves in a stratified half space. *Geophys. J. R. Astr. Soc.*, **57**, 557-583.

Kravstov Yu.A. and Orlov Y.I., 1990. *Geometrical Optics of Inhomogeneous Media*. Springer Verlag, Heidelberg.

Kristek J., Moczo P., Irikura I., Iwata T. and Sekiguchi H., 1999. *The 1995 Kobe mainshock simulated by the 3D finite differences*. In: Irikura K. et al. (eds.), The Effects of Surface Geology on Seismic Motion, **Vol. 3**, Balkema, Rotterdam, 1361-1368.

Kurkjian A.L., Coates R.T., White J.E. and Schmidt H., 1994. Finite-difference and frequency-wavenumber modelling of seismic monopole sources and receivers in fluid-filled boreholes. *Geophysics*, **59**, 1053-1064.

Lafond C.F. and Levander A.R., 1990. Fast and accurate dynamic ray tracing in heterogeneous media. *Bull. seismol. Soc. Am.*, **80**, 1284-1296.

Lecomte I., 1996. Hybrid modelling with ray tracing and finite difference, *66th Ann. Internat. Mtg: Soc. of Expl. Geophys.*, 699-702.

Levander A.R., 1989. Finite-difference forward modelling in seismology. In James D.E., (Ed.), *The Encyclopedia of Solid Earth Geophysics: Van Nostrand Rheinhold*, New York, 410-431.

McLaughlin K.L. and Day S.M., 1994. 3D Elastic Finite Difference Seismic Wave Simulations. *Computers in Physics*, **8**, 656.

Moczo P., 1989. Finite-difference technique for SH-waves in 2-D media using irregular grids – application to the seismic response problem. *Geophys. J. Int.*, **99**, 321-329.

Moczo P., Bystrický E., Kristek J., Carcione J.M. and Bouchon M., 1997. Hybrid modelling of P-SV seismic motion at inhomogeneous viscoelastic topographic structures. *Bull. seismol. Soc. Am.*, **87**, 1305-1323.

Moczo P., Lucka M., Kristek J. and Kristekova M., 1999. 3D displacement Finite Differences and a Combined Memory Optimization. *Bull. seismol. Soc. Am.*, **89**, 69-79.

Novotný O., Zahradník J. and Tselentis G.-A., 2001. North-Western Turkey Earthquakes and the Crustal Structure Inferred from Surface Waves Observed in Western Greece. *Bull. seismol. Soc. Am.*, **91**, 875-879.

Opršal I., Pakzad M., Plicka V. and Zahradník J., 1998. *Ground motion simulation by hybrid methods*, In: Irikura K. et al. (eds.), The Effects of Surface Geology on Seismic Motion, **Vol. 2**, Balkema, Rotterdam, 955-960.

Opršal I. and Zahradník J., 1999. Elastic finite-difference method for irregular grids. *Geophysics*, **64**, 240-250.

Opršal I. and Zahradník J., 2002. 3D Finite Difference Method and Hybrid Modelling of Earthquake Ground Motion. *J. Geophys. Res.*, **107**, 10.1029/2000JB000082, 16 pp.

Pitarka A., 1999. 3D Elastic Finite-Difference Modelling of Seismic Motion Using Staggered Grids, with Nonuniform Spacing. *Bull. seismol. Soc. Am.*, **89**, 54-68.

Robertsson J.O.A. and Chapman C.H., 2000. An efficient method for calculating finite-difference seismograms after model alterations. *Geophysics*, **65**, 907-918.

Robertsson J.O., Levander A. and Holliger K., 1996. A hybrid wave propagation simulation technique for ocean acoustic problems. *J. Geophys. Res.*, **101**, 11225-11241.

Yoshimura C., Bielak J., Hisada Y. and Fernandez A., 2002. Domain reduction method for three-dimensional earthquake modelling in localized regions. Part II: Verification and applications. *Bull. seismol. Soc. Am.*, accepted.

Zahradník J. and Moczo P., 1996. Hybrid seismic modelling based on discrete-wave number and finite-difference methods. *Pure Appl. Geophys.*, **148**, 21-38.